Prior exposure of microbial communities to seawater reduces resilience but increases compositional and functional resistance to flooding events

Lewis C. Browett, Sharon Ruiz-Lopez, Hannah L. Mossman, Andrew P. Dean , Damian W. Rivett

Abstract

Storm surges, flooding, and the encroachment of seawater onto agricultural land are predicted to increase with climate change. These flooding events fundamentally alter many soil properties and have knock-on effects on the microbial community composition and its functioning. The hypotheses tested in this study were (1) that the extent of change (resistance) of microbial community functioning and structure during seawater flooding is a factor of pre-adaptation to the stress, and (2) if structure and function are altered, the pre-adaptation will result in communities returning to previous state prior to flooding (resilience) faster than unexposed communities. We chose a naturally occurring saltmarsh-terrestrial pasture gradient from which three elevations were selected to create mesocosms. By selecting these sites, we were able to incorporate the legacy of differing levels of seawater ingress and exposure. Mesocosms were submerged in seawater for 0, 1, 96- and 192-h, with half of the mesocosms sacrificed immediately after flooding, and the other half taken after a 14 day “recovery” period. The following parameters were monitored: 1) changes in soil environmental parameters, 2) prokaryotic community composition, and 3) microbial functioning. Our results indicated that any length of seawater inundation significantly altered the physicochemical properties of all the soils, although a greater change is observed in the pasture site compared to the saltmarsh sites. These changes remained following a recovery period. Interestingly, our results indicated that for community composition, there was a high degree of resistance for the Saltmarsh mesocosms, with the Pasture mesocosm displaying higher resilience. Further, we observed a functional shift in the enzyme activities with labile hemicellulose being preferentially utilised over cellulose, with the effect increasing with longer floods. These results suggest that changing bacterial physiology is more critical to understanding the impact of storm surges on agricultural systems than bulk community change.

1. Introduction

Anthropogenic induced climate change is causing an amplification of storm surges as a result of continued sea-level rise (SLR) and increased storminess (Slangen et al., 2016). As storm surges increase in frequency and intensity, a rise of seawater flooding events across the planet have been observed (Narayan et al., 2017; Somboonna et al., 2014). These storm surges can breach coastal defences, resulting in flooding of low-lying areas inland with costly environmental, economic, and social consequences (Cheikh and Momen, 2020; Kim, 2019). Predictions show that annual sea flood damage will increase with SLR, with estimates in excess of $100 bn yr^{-1} depending on the country's coastal borders (Brown et al., 2021). Whilst the broad implications of seawater inundation are clear, flooding has specific consequences on the biotic component of ecosystems, particularly that of agricultural land.

Saline flooding of agricultural land has multiple effects. Flooding results in waterlogged, anoxic soils, and after the flood recedes salt deposits leave a legacy of salinized soil, affecting crop growth in the long term (Glenn et al., 1998; Randle-Boggis et al., 2018; Warrence et al., 2002). The effects of soil salinisation on the growth of crops and other terrestrial plants is well established, although the combined effects of salinity and flooding is less well known (Gould et al., 2020; Hanley et al., 2020). Key to potential mitigation of these impacts are understanding the ecology of the below-ground microbial components of these systems, disruption of which can have dramatic consequences for above-ground biomass (Meena et al., 2017).

The influx of seawater and the resulting increase in salinity, and decrease in oxygen potential, are both stressors to microbial communities. Changes in microbial biodiversity are routinely observed during periods of stress (Berga et al., 2017; Mombrikotb et al., 2022), however, the effect of the overall functionality of the community has been less-thoroughly addressed. Sudden inundation and an increase in salinity could disrupt key functions (Hanley et al., 2020), with prolonged flooding

leading to anoxic conditions which impacts soil enzyme activity and microbial nutrient cycling (Chambers et al., 2016; Chaudhary et al., 2016; Fitch et al., 2022; Wright et al., 2015). As such, it is vital to know the potential for communities that are likely to flood to resist these stresses and, if they are impacted, their resilience or potential for recovery (Shade et al., 2012).

The extent to which microbial communities can resist or recover from environmental change can, however, be dependent on prior exposure to the stress (Allison and Martiny, 2008; Shade et al., 2012). Fringing coastal habitats, such as saltmarshes, are adapted to regular saline inundation. However, saltmarshes are exposed to varying tidal inundation down the shore, which leads to zonation of species in adaptation to the specific conditions (Lee et al., 2016). Across a gradient from saltmarsh to terrestrial agricultural soils, frequent, prolonged inundation is common at lower elevation saltmarshes, but less so in coastal agricultural land due to higher elevation or sea defences.

In this study, we used an experimental mesocosm approach where sediments from Saltmarshes at low and high shore elevation, and pasture soils physically separated from high tides, were subjected to seawater flooding of 0, 1, 96 and 192 h duration. Environmental, microbial community, and functioning parameters were measured at the end of the flooding period, and 14 days followed the removal of the flooding. The aim of this study was to understand the environmental, and microbial compositional and functional changes caused by differing durations of seawater flooding, and whether prior exposure to seawater inundation mitigated the extent of change.

1.1. Objectives

- 1.

Determine the impact of increasing flooding duration on physicochemical parameters (pH, moisture, C:N ratio, and metal concentrations) at each elevation and the ability of the system to return to its initial state following removal of stress

- 2.

Determine the extent to which flooding duration changes bacterial community structure at each elevation, and whether further changes occur following removal of the flooding stress

- 3.

Determine how bacterial functioning (metabolic potential and carbon cycling enzymes) responds to flooding duration, and the ability of the community to regain function when flooding abates.

- 4.

Determine whether previous exposure to flooding increases the resistance of a mesocosm to change and, in the event of a change, increases the resilience of the system to return to the pre-flooded state after removal of the seawater.

2. Materials and methods

2.1. Sampling site

Soil samples were taken from three sites, two saltmarsh and one agricultural pasture site, located at RPSB Marshside, Southport, UK (Fig. S1). The two saltmarsh sites were chosen to be at different elevations and thus a different frequency of exposure to sea water inundation: the "low" elevation was at 4.37 m above ODN (equivalent of mean sea level, 53°40'44.4"N, 2°59'31.2"W) compared to the "high" elevation at 4.78 m ODN (53°40'37.2"N, 2°59'13.2"W). The level of mean high water spring tides at the nearest town (Southport) is 4.1 m ODN and the level of the highest astronomical tides is 5.0 m ODN, indicating that the low site is inundated by the tide <100 times per year and the high site <20 times per year. Finally, cattle grazed pasture located landward of the saltmarsh area behind a sea defence was also sampled (53°39'59.98"N, 2°59'27.91"W). This area has not been flooded with seawater since the establishment of a sea wall in 1959 but is located close to the sea and may have experienced some spray. Vegetation at the low elevation site was dominated by *Puccinellia maritima* and *Spartina anglica*. At the high elevation site *Festuca rubra* and *Agrostis*

stolonifera dominated, whereas the pasture site was dominated by species typical of neutral grasslands including *Lolium perenne* and *Trifolium repens*. The saltmarsh samples at both sites consisted of a sandy marine sediment, with a sandy loam soil at the pasture site.

2.2. Sampling

Soil core and seawater samples were taken on the 30th September 2020, with 20 l of seawater collected from an inlet into the saltmarsh (53°40'37.2"N, 2°59'31.2"W; Fig. S1). Prior to soil core collection, vegetation was trimmed by hand to ~1 cm. At each site, 24 cores of the top surface soil (0–5 cm depth), including any plants and roots present, were taken using a modified syringe (1.5 cm diameter). This syringe housing acted as both a corer, and as the mesocosm housing (Fig. S2) for the duration of the experiment. All samples were kept on ice and returned to Manchester Metropolitan University within 24 h, and placed into the on-site greenhouses where they were left for four days to acclimatise to the conditions.

2.3. Experimental design

This mesocosm experiment simulated different durations of flooding at each of the sites, together with a 14-day recovery period (Fig. 1). This allowed us to determine the extent to which seawater flooding changes microbial community structure and function, and, if changed, the community's ability to revert to a pre-flooded state. Destructive sampling was used in this experiment to avoid disrupting the soil and microbiome structure prior to processing samples for environmental and community analysis (Lombard et al., 2011). A total of 72 mesocosms were created for this experiment, comprising the 24 samples collected from each of the three sites. Six mesocosms from each site were subjected to one of four flooding duration; no flooding (control), one hour, 96 h (four days), and 192 h (eight days). At the cessation of flooding, half of the samples (n = 3) from each treatment were destructively sampled, with the other set (n = 3) drained and left for a 14 day "recovery" period before also being destroyed for analysis. For destructive sampling all mesocosms were drained of excess seawater before being ejected from the housing into an individually labelled

Ziplock bag and homogenised by hand. After homogenisation, the samples were measured for environmental parameters, ecosystem functions, and DNA extracted for community composition analysis.

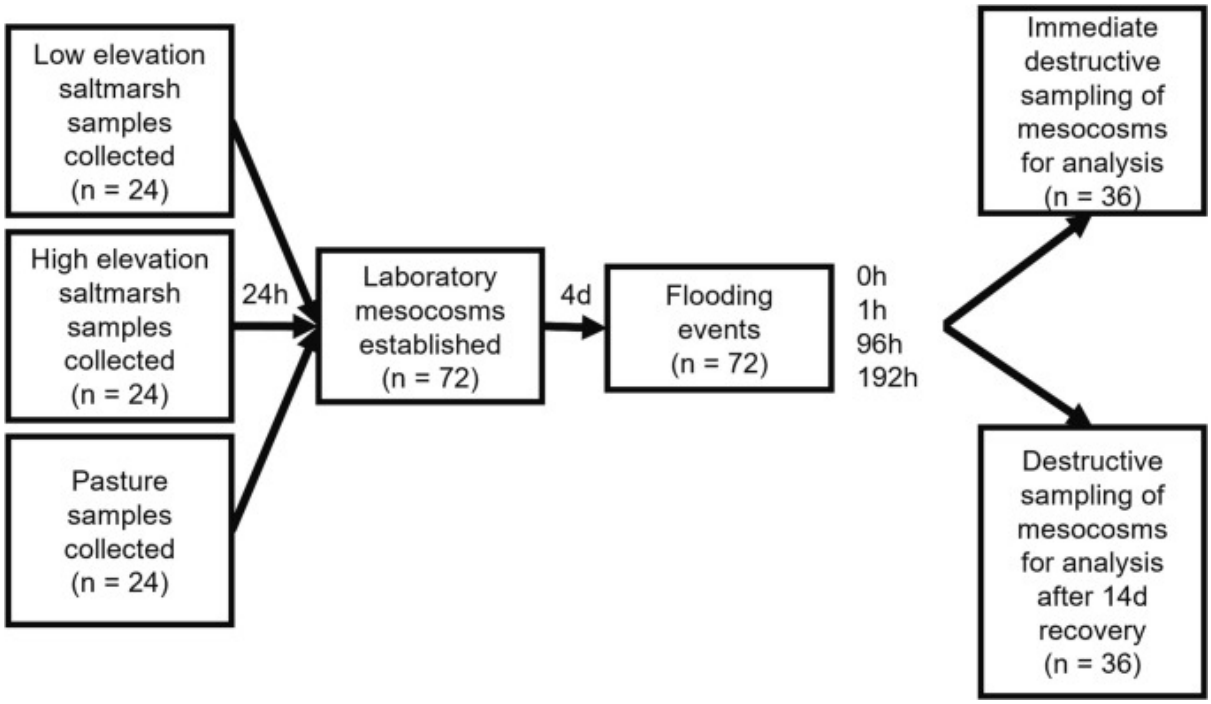

Fig. 1. Schematic of the experimental design. At each of the three sites, 24 samples were collected, each sample becoming an independent mesocosm. After four days these were subjected to different durations of flooding; a "0 h" control and 1 h, 96 h and 192 h. At the cessation of flooding, half the samples were immediately analysed, while half was left for 14 days before sampling.

2.4. Measurement of environmental parameters

To understand the impacts of seawater inundation on the physicochemical profile of the soil, multiple characteristics were measured. Mesocosms were destructively sampled before flooding (Time = 0 h) and immediately after three flooding durations (Time = 1, 96 or 192 h). To analyse changes in the soil pH and conductivity 1 g of soil was combined with 9 ml of deionized water in a plastic universal tube to create a 1:10 dilution. The mixture was shaken for 5 min and left to settle for 30 min. Conductivity was measured first using a Jenway 4510 Conductivity probe calibrated to

1413 µS and then pH measured with a Jenway 3510 pH probe calibrated using pH 7 and pH 10 buffers.

To enumerate the moisture content, 1–2 g of homogenised soil sample was weighed (soil wet weight) before drying at 105 °C for 24 h (Elmholt et al., 2000). Dry weights were then recorded and moisture content was calculated as a percentage (% w/w). Following the drying step, samples were refined to a uniform consistency with a pestle and mortar and split for analysis for carbon, nitrogen, and metal analysis.

For the Carbon: Nitrogen quantification, a subsample of 0.01 g was analysed through dry combustion by mass spectrometry analysis (*Elementar Vario* EL analyser). Inductively Coupled Plasma Optical Emission Spectroscopy (ICP-OES) was used to quantify trace elements (Al, As, Co, Cr, Cu, Ni, Pb, Zn,), seawater elemental composition (Mg, Na, Ca, K, S) as well as other elements (Fe, Mn, P). Dried samples (0.025 g) were broken down using microwave digestion by placing the sample into a clean, sealed, PTFE digestion vessel with 10 ml trace metal-grade nitric acid. After digestion, the contents of the vessels were gravity filtered through a 0.45 µm filter and the volume of the filtrate made up to 100 ml with deionized water. Seawater elemental composition (to understand the elements introduced *via* inundation) was determined by filtering 20 ml of seawater sample through a 0.45 µm syringe filter into a falcon tube and acidified to 2% acid with HNO_3. All metal determinations were the average of three technical repeats, and carried out on an iCAP 6000 Series ICP spectrometer (Thermo Scientific, UK).

2.5. Ecosystem function measurements

Microbial communities were detached from the soil matrix by washing the soil in Phosphate buffer solution (PBS; Sigma-Aldrich) following the procedure described in (Mombrikotb et al., 2022). Briefly, 1 g of soil sample was combined with 2 ml of Phosphate buffer solution (PBS) in a sterile bijoux tube, vortexed for 5 min, and allowed to settle until a layer of supernatant forms. The supernatant was

then removed for downstream processing. Viable cells were enumerated by ten-fold serial dilution, in PBS, plated onto Tryptone Soy Agar (TSA; Oxoid Ltd.), and incubated at 22 °C for four days.

Extracellular enzyme activity was measured from the mesocosms using substrate analogues fluorescently labelled with 4-methylumbelliferone (MUB; Sigma-Aldrich) as previously described (Rivett et al., 2016) to measure the cleavage of MUB from two specific substrates targeting xylase (4-MUB-β-D-xylopyranoside; Sigma-Aldrich) and cellulase enzymes (4MUB-β-D-glucopyranoside; Sigma-Aldrich) as described in (Sinsabaugh et al., 1991). Finally, the metabolic potential (accessible energy present within the system) was measured by monitoring total adenosine triphosphate (ATP) concentrations using the BacTitre Glo™ Cell Viability Assay (Promega Ltd.) as previously described (Rivett et al., 2016).

2.6. Analysis of prokaryotic community composition

DNA was extracted from 0.135 g of homogenised mesocosm soil using the Quick-DNA™ Faecal/Soil Microbe Miniprep Kit (ZYMO Research, CA, USA), following the manufacturers protocol. Community composition was assessed by sequencing the V4 region of the 16S rRNA gene on a MiSeq platform (Illumina, San Diego, CA, United States) using the dual indexing method (Kozich et al., 2013). Amplification from each sample was achieved using primers 515F and 806R (Caporaso et al., 2012) by pooling two independent amplification reactions prior to a separate reaction to attach the Illumina adaptors. Purification of the PCR products was performed using the AMPure XP magnetic beads treatment (Beckman Coulter, Indianapolis, IN, USA) on a ratio of 0.8, and the concentration of PCR purified products was measured using a Qubit 2.0 Fluorometer (ThermoFisher, Scientific) and normalised with SequalPrep Normalization Plates (ThermoFisher Scientific). The sequencing data were processed using the QIIME2 software package version 2020.8 (Bolyen et al., 2019). Raw amplicon data were processed using the DADA2 pipeline to create amplicon sequence variants (ASVs) present in each sample (Callahan et al., 2016). Sequences below 220 bp in length and an average quality score below 30 on a window of 20 bases were discarded. Taxonomy of the ASVs was

assigned using a Naïve-Bayes approach implemented in the SILVA database (Quast et al., 2013). ASVs were condensed to phylotypes (highest taxonomic identification) based on the taxonomic alignment (Rivett and Bell, 2018). The sequencing yielded 361,669 reads with a mean of 6458 ± 706 (1 s.e.m.) reads per sample, with rarefaction curves indicated that the diversity was adequately sampled in the majority of mesocosms (Fig. S3). Those that had not plateaued (n = 4), or those with <10 taxa identified (n = 12), were excluded from further analysis, which included all replicates for the low saltmarsh mesocosms flooded for 96 h. Sequences are deposited under the SRA accession number PRJNA796483.

2.7. Determination of resistance and resilience

The resistance (RS) and resilience (RL) indices were calculated to assess the microbial response to the disturbance. Both indices were calculated for alpha diversity, and enzymatic activity. RS and RL indices were calculated using the following expressions (Orwin and Wardle, 2004):RS=1−2Co−PoCo+Co−PoRLx=2Co−PoCo−Po+Cx−Px−1where Co and Po are the values of the variables in the control and recovery samples, respectively, x represents the duration of flooding, and Cx – Px represent the difference between the control at time x (Cx) and the disturbed soil at time x (Px). The values of both indices ranged between −1 and + 1. For measures of resistance +1 represents the maximal resistance (*i.e.* unchanged), and − 1 represents a total destruction of the measure. For measures of resilience, +1 indicates a return to the original, pre-stressed, state, with −1 indicating a change to a stable alternative state.

2.8. Statistical analysis

Three-way analysis of variance (ANOVA) was conducted on all variables with Site (Low Saltmarsh/High Saltmarsh/Pasture), Recovery (post-flood/post-recovery period), and Flooding Duration (as a categorical variable of 0/ 1/ 96/ 192 h) included as explanatory variables with all the interactions. To allow for direct comparisons between all response variables, all non-significant interactions were retained. To mitigate the order of the variables affecting the analysis, all ANOVA

were performed with a type III error structure using the "car" package (Fox and Weisberg, 2019). Normality of errors and homogeneity of variances were assessed visually prior to undertaking the analysis. Where required, data were logarithm (base 10) transformed to conform with the assumptions for parametric statistics. *Per capita* measures of functions (metabolic potential and enzyme activity) were calculated by dividing the functional measurement by the viable bacterial count (Rivett et al., 2016).

Comparisons of community diversity between treatments using univariate and multivariate methods were undertaken. Fisher's alpha was used as the measure of richness, and Simpson's (1-*D*) was a measure of dominance. Neither of these measures are affected by sample size at the sampling depth observed here, so no rarefaction or bootstrapping of the sequence data was performed (Rogers et al., 2013). Multivariate environmental and community data were visualised using ordination plots with either Principal Component Analysis (using natural logarithm transformed data (Aguinaga et al., 2018)) or Nonmetric Multidimensional Scaling (NMDS) using Bray-Curtis dissimilarity index respectively. Permutational Multivariate ANOVA (PERMANOVA) and analysis of similarity (ANOSIM) were performed to analyse the impact of the environmental variables on compositional data. All statistical analyses and visualisations were performed in R (v4.1.2) (R, 2020) statistical environment. ANOSIM, NMDS and PERMANOVA were performed using the vegan package (Oksanen et al., 2019).

3. Results

3.1. Environmental parameters: pH, conductivity, moisture content & C:N ratio

The mesocosms were analysed for conductivity, moisture, C:N ratio and pH. At the start of the experiment (no flood control; Fig. 2, light coloured bars at time 0), there was a decrease in conductivity across elevation with the Low Saltmarsh (mean ± 1 s.e.m. throughout, 6.54 ± 0.54 mS), the High Saltmarsh (5.40 ± 0.71 mS) or the Pasture site (4.35 ± 0.41 mS) which was found to be non-significant ($F_{2,6}$ = 3.74, p = 0.088; Table S1). Contrary to this, the analyses for moisture content found significant differences ($F_{2,6}$ = 18.75, p = 0.003) with Tukey's post-hoc tests showing the High

Saltmarsh site (65.25 ± 2.86%) as significantly (Low-High p_{adj} = 0.011; Pasture-High p_{adj} = 0.003) wetter than the Low Saltmarsh (48.59 ± 0.92%) and the Pasture site (42.68 ± 3.59%), which were not significantly different from each other (p_{adj} = 0.337). Significant differences ($F_{2,6}$ = 53.72, p < 0.001; Table S1) were also observed in C:N ratio, with the Pasture site (11.19 ± 10.79) shown to be significantly lower (Pasture-High p_{adj} < 0.001, Pasture-Low p_{adj} < 0.001) than the Low (14.08 ± 13.56) and High Saltmarsh (14.09 ± 13.65) sites, between which no difference was observed (p_{adj} = 0.999). A similar pattern was observed in the pH values with the significant differences between sites ($F_{2,6}$ = 14.38, p = 0.005; Table S1) driven by the Pasture site (6.96 ± 0.04; Pasture-High p_{adj} = 0.049, Pasture-Low p_{adj} = 0.004) being lower than the Low (7.66 ± 0.14) and High (7.68 ± 0.06) Saltmarsh sites, which were not significantly different (p_{adj} = 0.141).

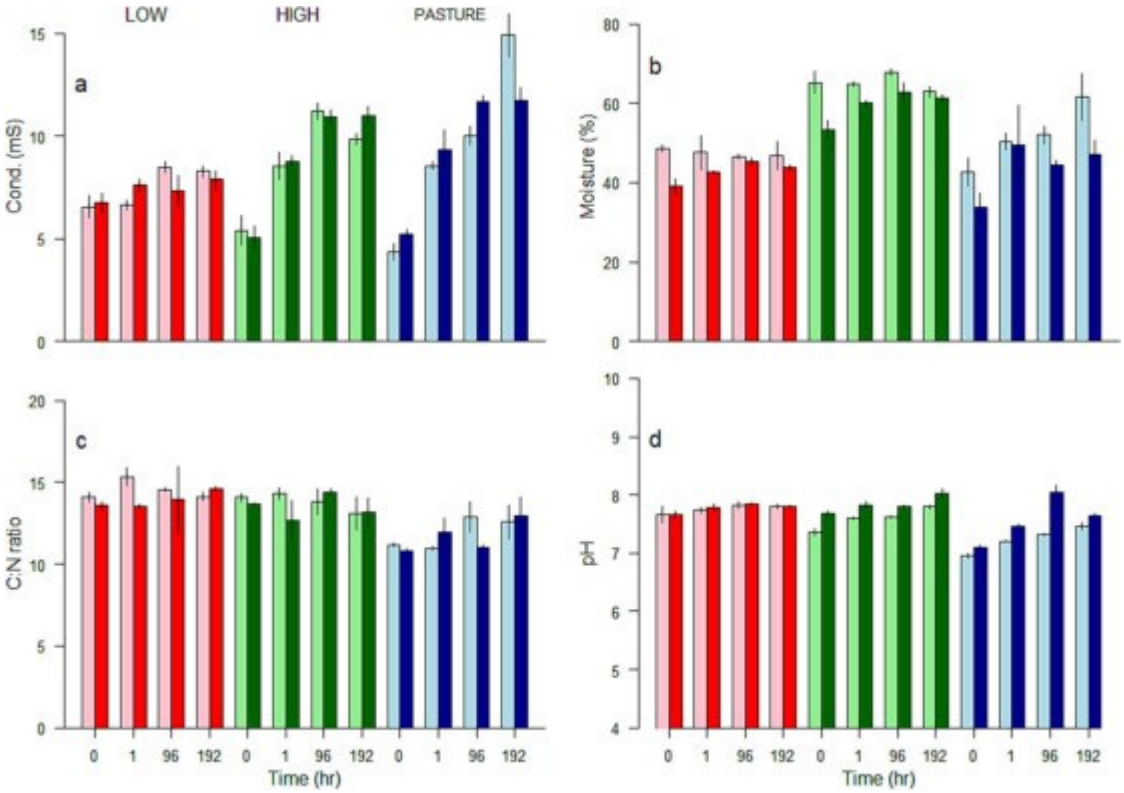

Fig. 2. Changes in (a) conductivity (b) moisture content, (c) C:N ratio and (d) pH in mesocosms established from sediments from low (red), and high (green) salt marsh sites and pasture (blue). Readings were taken immediately after flooding of various durations (light colour bars), and after

14 days of recovery (darker bars). Each bar represents the mean of independent replicate mesocosms (n = 3). Error bars represent ±1 sem.

With increased flooding duration, the conductivity increased significantly across all sites ($F_{3,48}$ = 22.99, p < 0.001; Fig. 2a, light bars; Table S1), however, the extent of change altered depending on the site (Time x Site: $F_{6,48}$ = 15.28, p < 0.001) with the extent of change increasing moving from Low to High Saltmarsh to Pasture. With respect to moisture content (Fig. 2b, light bars), no overall difference was observed with increasing flooding duration; the moisture content in the Pasture site increased with flooding duration which was not, however, observed in either of the Saltmarsh sites (Time x Site: $F_{6,48}$ = 2.55, p = 0.032). There was no effect of flooding duration on C:N ratio across any of the sites (Fig. 2c, light bars), however, pH (Fig. 2d, light bars) increased significantly ($F_{3,48}$ = 10.13, p < 0.001) with increased flooding duration with this effect being more pronounced in the Pasture mesocosms.

Despite a significant effect in conductivity with increased flooding duration, there is little evidence that these values changed over the 14-day "recovery" period (Fig. 2a, dark bars; $F_{1,48}$ = 0.22, p = 0.641; Table S1). The moisture content (Fig. 2b, dark bars) of the mesocosms was significantly ($F_{1,48}$ = 6.83, p = 0.012) lower after the recovery period than when flooded, regardless of duration. No differences were observed in C:N ratio (Fig. 2c, dark bars), but pH (Fig. 2d, dark bars) had significantly ($F_{1,48}$ = 15.61, p < 0.001) higher values overall after the recovery period, with the effect significantly increasing (Time x Site x Recovery State: $F_{6,48}$ = 4.61, p = 0.001) from Low to High Saltmarsh to Pasture.

3.2. Environmental parameters: metal concentration

The elemental content of the soils was characterised (Fig. 3, light coloured bars at time 0; Supplementary Fig. 4). In the no flood controls, our analysis found significant differences between the sites for Ca ($F_{2,6}$ = 41.24, p < 0.001), K ($F_{2,6}$ = 94.37, p < 0.001), Mg ($F_{2,6}$ = 166.65, p < 0.001), Na ($F_{2,6}$ = 42.74, p < 0.001), Fe ($F_{2,6}$ = 106.18, p < 0.001) and P ($F_{2,6}$ = 100.11, p < 0.001). For all the

metals, the concentrations were significantly lower (p_{adj} < 0.001 in all cases) in the Pasture sites (Ca: 6.87 ± 0.66 mg/g, K: 0.57 ± 0.06 mg/g, Mg: 1.38 ± 0.09 mg/g, Na: mg/g, Fe: 4.65 ± 0.07 mg/g, P: 0.51 ± 0.01 mg/g) than in either the Low Saltmarsh (Ca: 34.44 ± 3.43 mg/g, K: 3.38 ± 0.14 mg/g, Mg: 13.84 ± 0.84 mg/g, Na: 7.27 ± 0.36 mg/g, Fe: 27.07 ± 1.37 mg/g, P: 0.95 ± 0.04 mg/g) or High Saltmarsh sites (Ca: 18.17 ± 1.33 mg/g, K: 4.02 ± 0.29 mg/g, Mg: 14.15 ± 0.49 mg/g, Na: 9.49 ± 0.85 mg/g, Fe: 26.32 ± 1.64 mg/g, P: 1.10 ± 0.03 mg/g). Only Ca (p_{adj} = 0.004) and P (p_{adj} = 0.035) showed significant differences between the Saltmarsh sites.

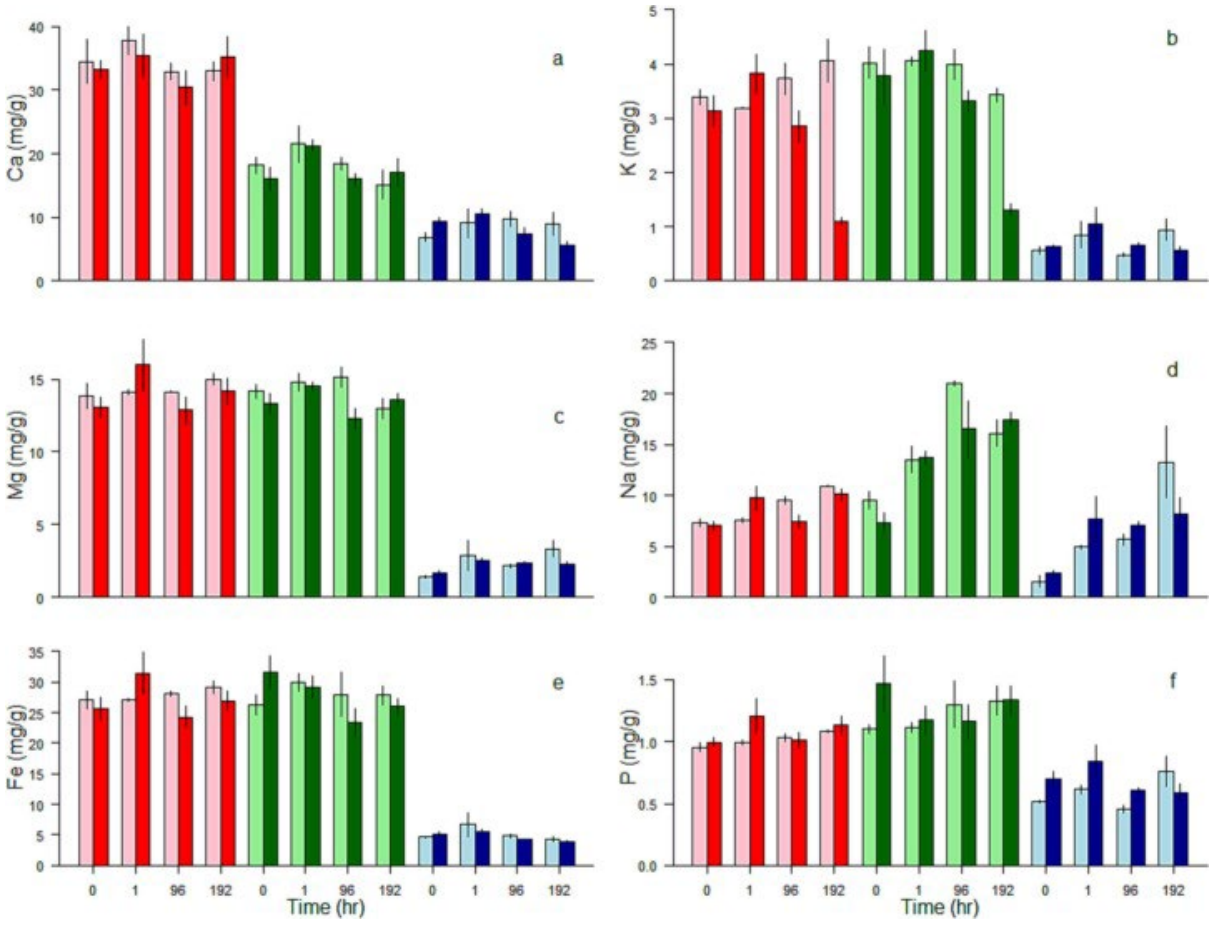

1.

Fig. 3. Concentration of selected metal ions (a-f) within the mesocosms from low (red), and high (green) salt marsh sites and pasture (blue). Readings were taken immediately after flooding of various durations (light colour bars), and after 14 days of recovery (darker bars). Each bar represents the mean of independent replicate mesocosms (*n* = 3). Error bars represent ±1 sem.

When the impact of flooding duration was analysed against each of the metals, only Na (Fig. 3D, light bars) indicated a significant overall increase with prolonged flooding ($F_{3,48}$ = 15.16, p < 0.001), with the Pasture and the High Saltmarsh sites more impacted than the Low Saltmarsh site (Time x Site: $F_{6,48}$ = 5.79, p < 0.001) for metals K ($F_{6,48}$ = 8.91, p < 0.001; Fig. 3b, light bars) and Fe ($F_{6,48}$ = 3.05, *p* = 0.038; Fig. 3e, light bars).

Significant differences in Fe ($F_{1,48}$ = 4.88, *p* = 0.032) and P ($F_{1,48}$ = 7.23, *p* = 0.010) were observed after the recovery period (Fig. 3e & f, dark bars, respectively) compared to the flooded values, however, these differences did not have a clear overall trend, and fluctuated depending on the flooding duration for Fe (Time x Recovery: $F_{3,48}$ = 3.05, p = 0.038). This time dependent change after recovery was also significant for K (Time x Recovery: $F_{3,48}$ = 8.91, p < 0.001; Fig. 3b, dark bars) with the concentration of K lower with prolonged flooding. This trend was increasingly pronounced going from Pasture to High to Low Saltmarsh (Time x Site x Recovery: $F_{6,48}$ = 3.69, *p* = 0.004). This three-way interaction of flooding duration and site after the recovery period also influenced the Na concentration ($F_{6,48}$ = 3.69, *p* = 0.04; Fig. 3d, dark bars), where the Low Saltmarsh site displayed the least change regardless of the treatment.

When the composition of the metals was analysed using a permutation ANOVA (PERMANOVA), significant changes in metal composition were observed with increasing flooding duration (PERMANOVA $F_{3,48}$ = 10.32, *p* = 0.001, R^2 = 0.03), with this change dependent on site (PERMANOVA $F_{6,48}$ = 3.80, *p* = 0.002, R^2 = 0.02). Overall, the composition of the metals was significantly altered after the recovery period, but the direction of change was dependent on the duration of flooding (PERMANOVA Time x Recovery: $F_{3,48}$ = 2.77, *p* = 0.048, R^2 = 0.01).

Principal Components Analysis (PCA) showed that the sites clustered according to physicochemical properties (Fig. 4); significant differences were identified overall between the sites (PERMANOVA $F_{2,6}$ = 134.78, *p* = 0.007), with the Pasture site significantly different from both Saltmarsh sites

(ANOSIM R = 0.1, p = 0.014), but no difference observed between the Saltmarsh sites (ANOSIM R = 0.963, p = 0.1, permutations = 719) .

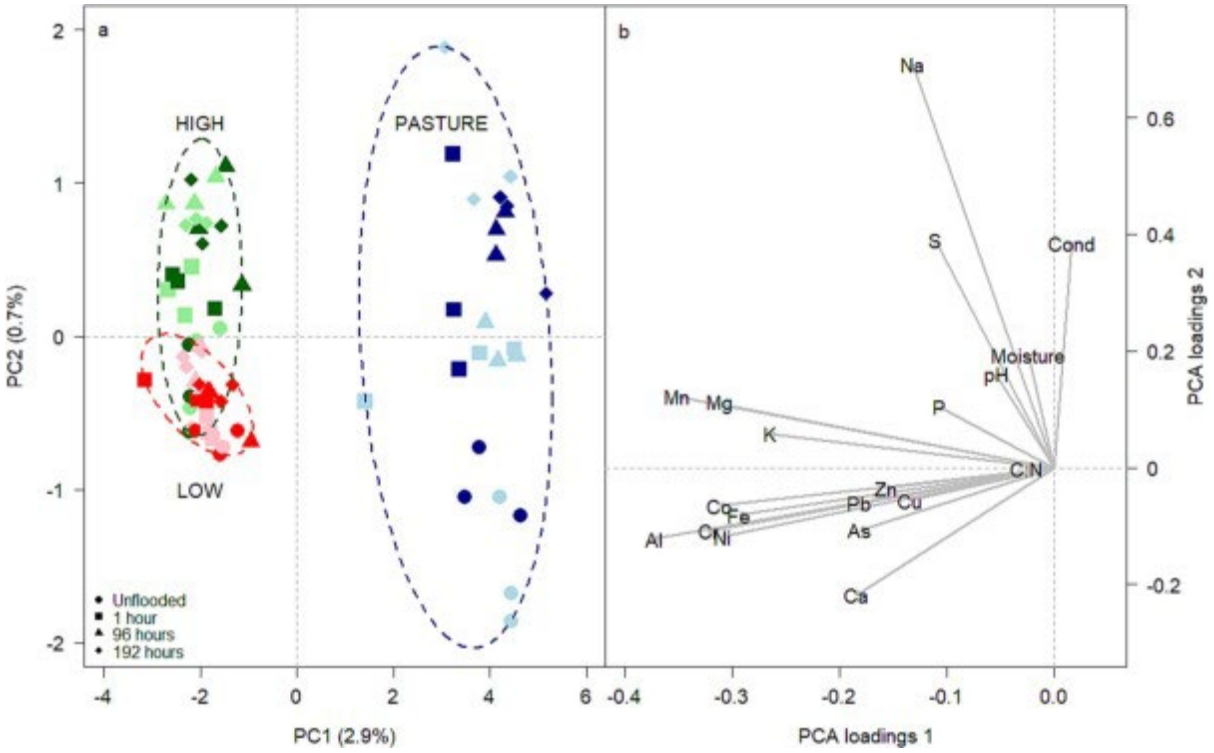

Fig. 4. Discrimination of sites and response to flooding based on physicochemical parameters. (a) Principal component analysis ordination plot and (b) a loading plot showing the extent of which each parameter contributes to the observed separation. Each point represents one mesocosm established from the Low (red) and High (green) saltmarsh and the Pasture (blue) soils. Lighter points indicate flooded mesocosms, whilst darker point represent mescocosms after recovery. Ellipses are used to denote the spread of the points for each site.

3.3. Microbial community structure: alpha diversity

The DNA extracted from each mesocosm was profiled using 16S rRNA gene amplicon sequencing. We calculated measures of community diversity to assess richness (Fisher's alpha) and community structure (Simpson's index). At the start of the experiment, the non-flooded controls were found to have significantly different species richness (Fig. 5a) between the sites ($F_{2,4}$ = 7.91, p = 0.041), with the Pasture site (51.50 ± 34.50 taxa) significantly lower that the Low Saltmarsh site (131.33 ± 7.36

taxa; p_{adj} = 0.038) but not the High Saltmarsh site (116.50 ± 14.5 taxa; p_{adj} = 0.102). No significant differences were observed between the two Saltmarsh sites (p_{adj} = 0.700). Similarly, there was a significant difference ($F_{2,4}$ = 7.40, p = 0.045) between the sites with respect to the community structure (Fig. 5b). There was no difference (p_{adj} = 0.896) between the Low (0.97 ± 0.001) and High (0.98 ± 0.001) Saltmarsh sites, however, the Pasture site was lower (0.92 ± 0.020) than both Saltmarsh sites albeit not significantly (Pasture-High p_{adj} = 0.056; Pasture-Low p_{adj} = 0.062).

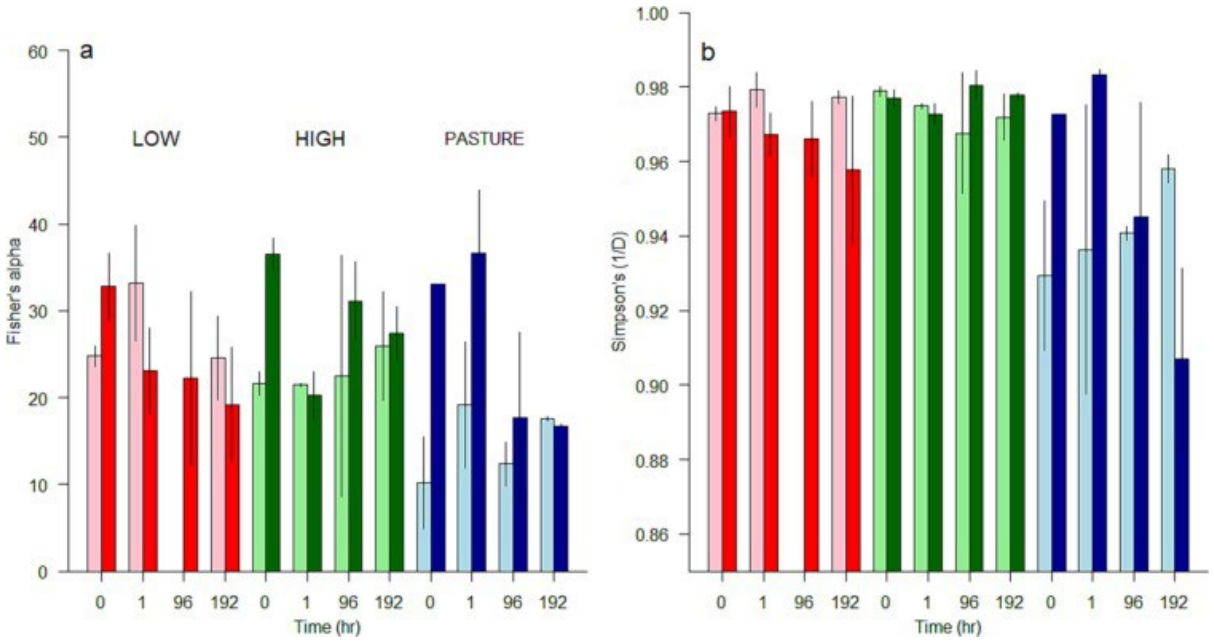

Fig. 5. Changes in (a) richness and (b) community structure of the bacterial communities present within the mesocosms. Compositions were taken immediately after flooding of various durations (light colour bars), and after 14 days of recovery (darker bars). Each bar represents the mean of independent replicate mesocosms (n = 3) established from the Low (red) and High (green) saltmarsh and the Pasture (blue) soils. Error bars represent ±1 sem.

No significant effect of increased flooding duration was observed for either species richness ($F_{3,33}$ = 0.15, p = 0.928) or community structure ($F_{3,33}$ = 0.09, p = 0.964). Neither were there any significant overall trends observed after the recovery period.

3.4. Microbial community composition: multivariate approaches

Multivariate analysis of the microbial community composition (Fig. 6) showed significant differences in β-diversity between the three sites (PERMANOVA $F_{2,6} = 2.67$, $p = 0.012$, $R^2 = 0.57$). Similar to the pattern seen in the PCA for physicochemical parameters (Fig. 4), there were no significant differences observed between the two Saltmarsh sites (ANOSIM $R = 0.42$, $p = 0.2$, permutations = 119), however, significance was observed between the Saltmarsh sites and the Pasture (ANOSIM $R = 0.89$, p = 0.045, permutations = 5039), with the Pasture site showing the least concentrated cluster, therefore more impacted, than the Low Saltmarsh site with the tightest cluster.

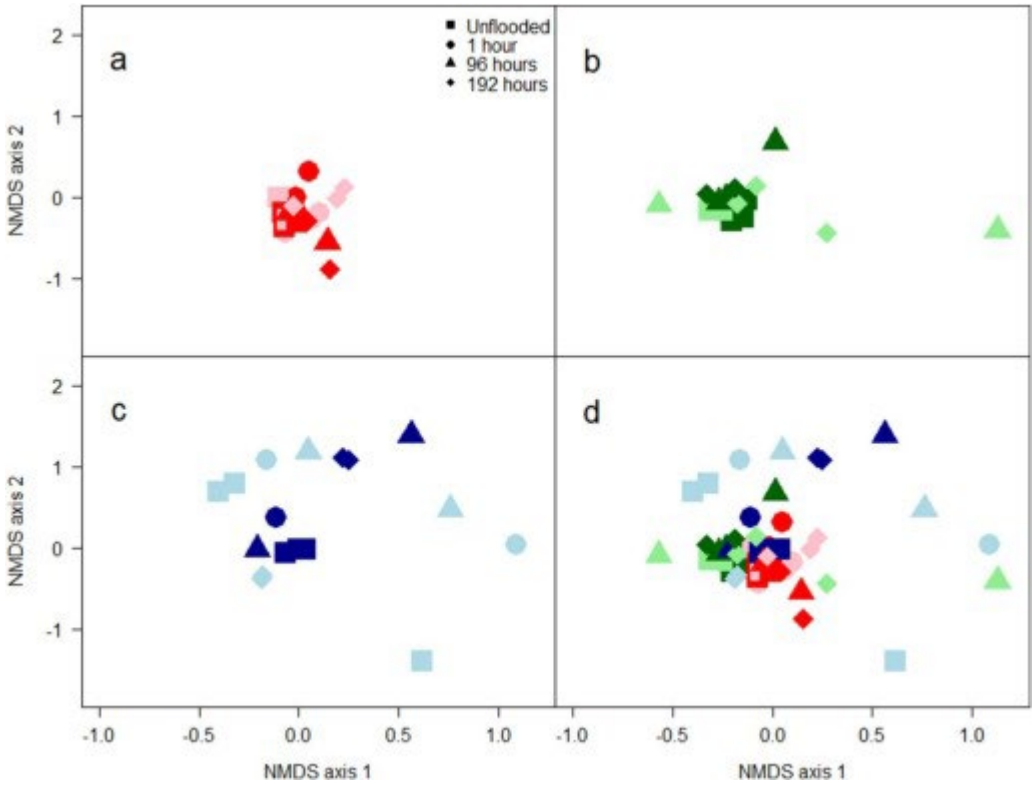

Fig. 6. Discrimination of sites and flooding response on the basis of bacterial community structure. Composition for (a) low, (b) high, and (c) pasture mesocosms were taken immediately after flooding of various durations (light colour points), and after 14 days of recovery (darker colours). Each point represents one mesocosm established from the Low (red) and High (green) saltmarsh and the Pasture (blue) soils. A composite image of the three sites is displayed for comparison (d).

There was a significant effect of increasing flooding duration on microbial composition (PERMANOVA $F_{3,33}$ = 1.83, p = 0.009, R^2 = 0.07; Table S2). The extent of change was significantly different depending on the site (PERMANOVA Time x Site: $F_{6,33}$ = 1.66, p = 0.004, R^2 = 0.12), where the Pasture site (Fig. 6c, light points) was observed to have the greatest degree of change due to flooding compared to the Saltmarsh sites (Fig. 6a & b, light points). Analysis of the abundance of the individual phylotypes (Fig. 7) highlighted that there was a greater degree of stochasticity in the Pasture site compared to either Saltmarsh sites during flooding events of all durations.

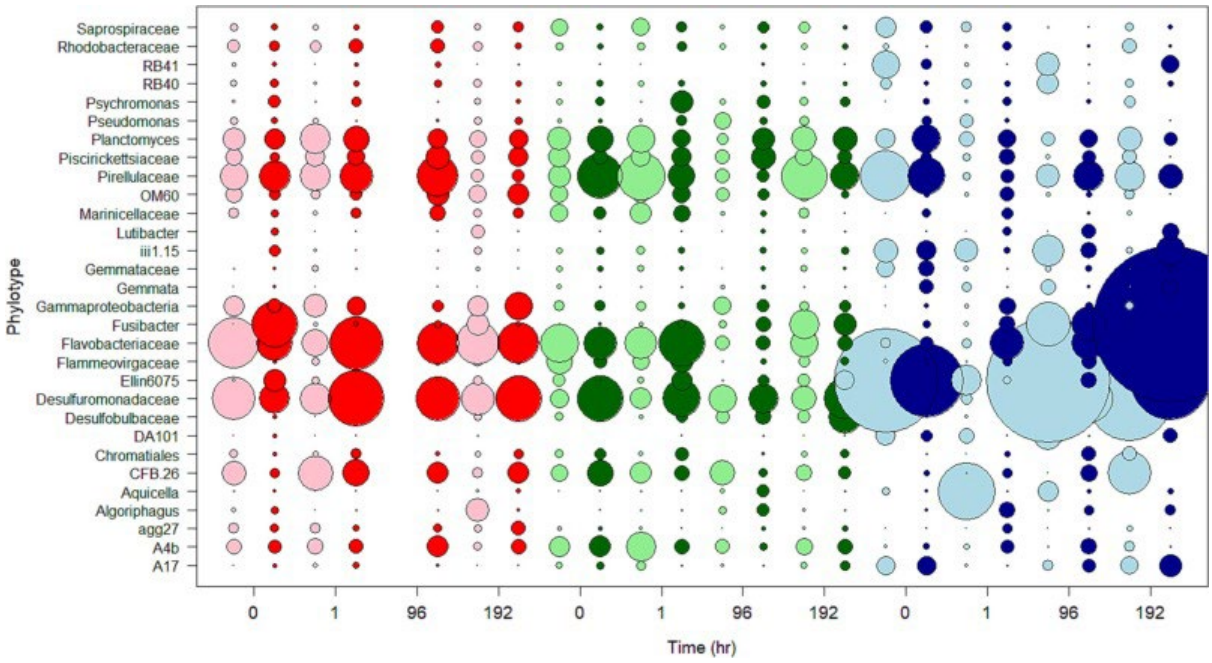

Fig. 7. Bubble plot indicating the variation of phylotypes within the mesocosms. The phylotypes presented are those with the greatest (top 5%) standard deviations across the entire dataset. The size of the points represents the mean (n = 3) relative abundance of the phylotype in the Low (red) and High (green) Saltmarsh, and Pasture (blue) sites across the flooded (light colours) and recovery (dark colours) periods.

Significant differences were observed after recovery (PERMANOVA Time x Recovery: $F_{3,33}$ = 1.75, 0.008, R^2 = 0.06) with longer flooding durations causing greater disruption in the composition (Fig. 6, dark points). Further, the degree of this impact was dependent on the site (PERMANOVA Time x Site

x Recovery: $F_{5,33}$ = 1.99, p = 0.003, R^2 = 0.12), with the Pasture site having a more disparate spread of compositions compared to the Saltmarsh sites. When focusing on the individual taxa, there was a strong but unpredictable response from those phylotypes in the Pasture site compared to those in the Saltmarsh sites (Fig. 7, dark circles).

3.5. Ecosystem functioning

In terms of ecosystem functioning, the viable cell counts, metabolic potential (ATP concentration), and the activity of enzymes required for carbon cycling were monitored for all mesocosms at each timepoint. At the start of the experiment, the analysis indicated significant differences between the sites (data not shown) for viable cell counts ($F_{2,6}$ = 5.68, p = 0.041) with a Tukey *post-hoc* test indicating that the High Saltmarsh site (376.44 ± 135.73 cfu g^{-1}) was significantly (p_{adj} = 0.043) lower than the Low Saltmarsh site (1008.00 ± 194.29 cfu g^{-1}). The Pasture site (422.00 ± 49.17 cfu g^{-1}) was not significantly different from either of the other two sites. Due to this significant difference, the following ecosystem functions (cellulase and xylase activity, and metabolic potential) were analysed as *per capita* values to avoid bias. As such, there was no significant differences in cellulase ($F_{2,6}$ = 0.57, p = 0.595) or xylase activity ($F_{2,6}$ = 2.80, p = 0.139) between the sites, however, significant ($F_{2,6}$ = 5.57, p = 0.043) differences were observed in metabolic potential. Here, contrary to pattern observed in the bacterial cell count data, the High Saltmarsh site (1.74 ± 0.46 nM ATP) was significantly (p_{adj} = 0.037) higher than either the Low Saltmarsh site (0.49 ± 0.09 nM ATP) or the Pasture site (1.07 ± 0.24 nM ATP).

For metabolic potential there was a significant ($F_{3,48}$ = 9.08, p < 0.001; Table S3) decrease in metabolic potential with increased flooding duration (Fig. 8a, light bars). Whilst each site decreased in metabolic potential, the degree of the decrease was different between the sites (Time x Site: $F_{6,48}$ = 2.92, p = 0.016).

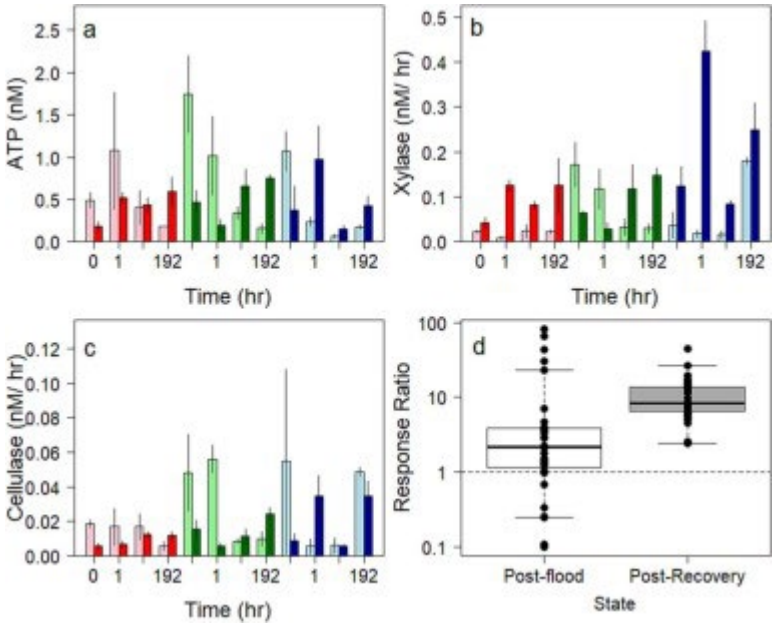

Fig. 8. Changes in *per capita* ATP concentration (a) xylase activity (b) and cellulase (c) activity were observed with flooding duration. Measurements were taken immediately after flooding of various durations (light colour bars), and after 14 days of recovery (darker bars). Each bar represents the mean of independent replicate mesocosms (n = 3) established from the Low (red) and High (green) saltmarsh and the Pasture (blue) soils. Error bars represent ±1 sem. Changes in substrate utilisation was analysed using a ratio of xylase: cellulase activity. Values were compared from immediately after the flood (white) to after the recovery period (grey; d).

As flooding duration increased there was a significant decrease in xylase activity ($F_{3,48}$ = 2.88, p = 0.045; Fig. 8b, light bars; Table S3), however, there were significant differences (Time x Site: $F_{6,48}$ = 4.02, p = 0.002) between how the sites reacted to increasing flood duration. Contrary to this, the cellulase activity (Fig. 8c, light bars) was not significantly influenced by flooding duration ($F_{3,48}$ = 2.71, p = 0.055), but each of the site did react differently ($F_{6,48}$ = 4.33, p = 0.001).

Only for the metabolic potential was a significant decrease observed between the flooded mesocosms, and those analysed after the 14-day recovery period ($F_{2,48}$ = 2.69, p = 0.016). Further, there was significant (Time x Site x Recovery: $F_{6,48}$ = 2.90, p = 0.017) differences in how metabolic

potential decreased with increased flooding duration for each of the individual sites (Fig. 8a, dark bars).

For both enzymes, the activity was not significantly altered after the recovery period. For xylase (Fig. 8b, dark bars), the impact of increasing duration significantly (Time x Recovery: $F_{3,48} = 4.02$, $p = 0.012$) changed from a decrease to an unclear trend across the different sites (Time x Site x Recovery: $F_{6,48} = 4.00$, $p = 0.003$). This result was reproduced with the cellulase activity (Time x Recovery: $F_{3,48} = 4.33$, $p = 0.029$; Time x Site x Recovery: $F_{6,48} = 2.96$, $p = 0.015$; Fig. 8c, dark bars), showing no clear overall trend to the activity of these enzymes. Interestingly, the overall ratio (xylase: cellulase activity) of the enzyme activities (Fig. 8d) significantly shifted to the utilisation of substrates degraded by xylase (paired $t_{35} = 0.67$, $p < 0.001$) after the recovery period.

3.6. Resistance and resilience

To understand the degree of change that flooding had on the different sites, indices of resistance and resilience were calculated. For resistance, all the mean values fell between 0 and 1, indicating that measures of richness (Fig. 9a), community structure (Fig. 9b) and ecosystem functioning (Fig. 9c-e) were either completely disturbed by the flooding (resistance = 0) or impervious (resistance = 1). For richness and community structure (Fig. 9a-b) measures, no significant differences observed between the sites (Kruskal-Wallis, Richness: $\chi^2_2 = 4.11$, $p = 0.128$; Simpson's $\chi^2_2 = 4.03$, $p = 0.134$). For the ecosystem functions (Fig. 9c-e), whilst no significant differences were observed between the sites (Kruskal-Wallis, cellulase: $\chi^2_2 = 3.47$, $p = 0.177$; xylase $\chi^2_2 = 2.4$, $p = 0.301$; metabolic potential: $\chi^2_2 = 0.63$, $p = 0.733$) due to the large variances detected, there was a clear trend with the Low Saltmarsh (cellulase: 0.61 ± 0.22; xylase: 0.65 ± 0.21; metabolic potential: 0.28 ± 0.23) site displaying a higher level of resistance than the High Saltmarsh (cellulase: 0.31 ± 0.20; xylase: 0.24 ± 0.14; metabolic potential: 0.19 ± 0.11) which was higher than the Pasture (cellulase: 0.30 ± 0.25; xylase: 0.00 ± 0.30; metabolic potential: 0.08 ± 0.03).

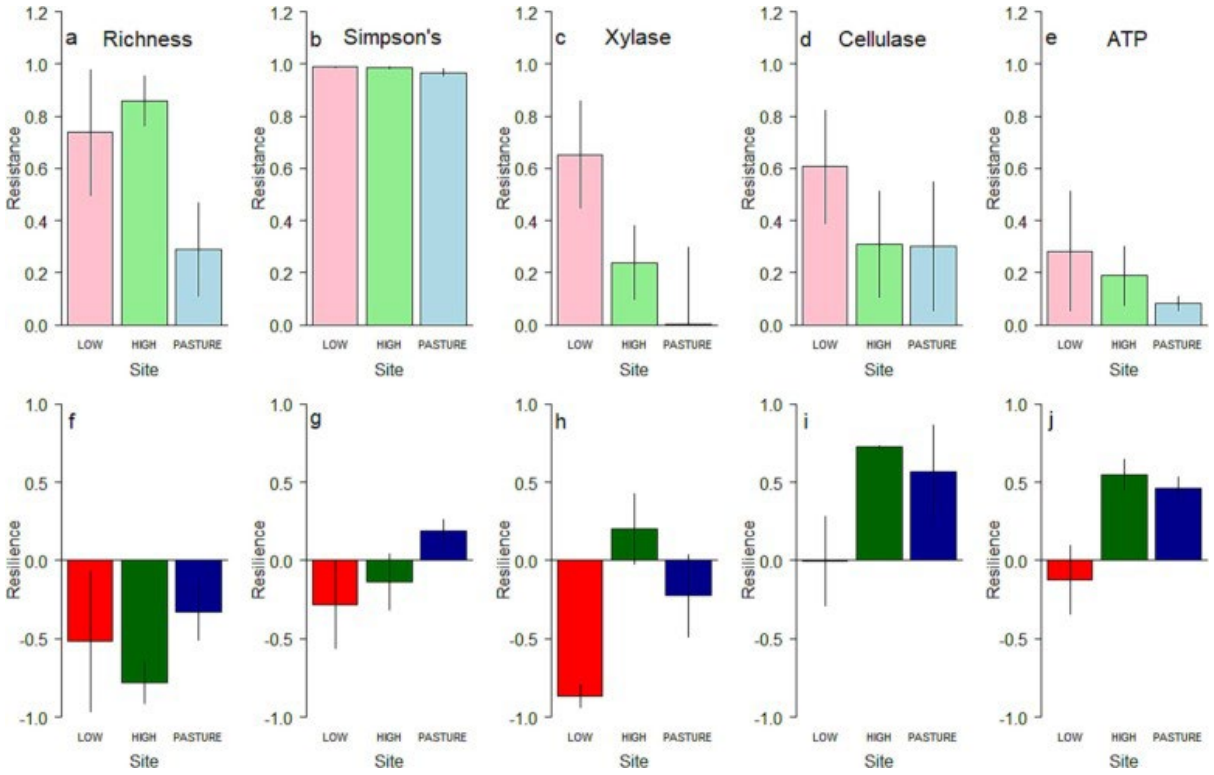

Fig. 9. Resistance (a-e) and resilience (f-j) indices for the different sites. The sites showed little difference in their ability to resist seawater inundation with respect to richness (a) and community structure (b). When focusing on functioning, however, there was a clear trend with xylase (c) and cellulase (d) activity, and metabolic potential (e) where the Low Saltmarsh site was more resistant to flooding than the other two sites, with the Pasture site being the least resistant. In terms of resilience, there were no significant differences between the sites for richness (f) and community structure (g), and for cellulase activity (i), however, for xylase (h) and metabolic potential (j) the Low Saltmarsh site was shown to be significantly lower. Each bar represents the mean of independent replicate mesocosms (*n* = 3) established from the Low (red) and High (green) saltmarsh and the Pasture (blue) soils. Error bars represent ±1 sem.

For measures of resilience (Fig. 9f-j), the mean values ranged between −1 and 1; this indicated that there was a range of reactions to the flooding events, with some communities recovering fully (Resilience = 1), not at all (Resilience = 0), or moving to an alternative state (Resilience = −1). Like the resistance index, no significant difference was found between the sites when investigating richness

(Kruskal-Wallis $\chi^2_2 = 2.23$, $p = 0.325$; Fig. 9f) or Simpson's (Kruskal-Wallis $\chi^2_2 = 4.03$, $p = 0.133$; Fig. 8g). For the function measures, there were differences in xylase resilience (Kruskal-Wallis $\chi^2_2 = 5.96$, $p = 0.051$; Fig. 9h), particularly between ($p_{adj} = 0.043$) the Low (−0.87 ± 0.07) and High (0.20 ± 0.22) Saltmarsh sites, with the Pasture site having a negative resilience value between the Saltmarsh sites (−0.22 ± 0.26; Pasture-Low $p_{adj} = 0.057$, Pasture-High $p_{adj} = 0.972$). In contrast, there was no significant difference between the sites (Kruskal-Wallis $\chi^2_2 = 3.29$, $p = 0.193$); however, the Low Saltmarsh site was lower (−0.01 ± 0.28) than the High Saltmarsh (0.72 ± 0.01) and Pasture (0.57 ± 0.29) sites. Finally, the metabolic potential (Fig. 8j) showed differences between sites (Kruskal-Wallis $\chi^2_2 = 5.42$, $p = 0.066$) in the same manner as the xylase activity; there were significant differences between the Low (−0.12 ± 0.22) and High (0.55 ± 0.10; $p_{adj} = 0.043$) with the resilience of the Pasture (0.46 ± 0.07) situated in between (Pasture-Low $p_{adj} = 0.057$; Pasture-High $p_{adj} = 0.972$).

4. Discussion

The aim of this study was to understand the environmental and biological changes caused by the inundation of terrestrial habitats with seawater for increasing durations. We hypothesised that Saltmarsh communities will have higher resistance to inundations and, if changed, have greater resilience to recover to the previous community composition and function prior to inundation. Further to this, this study set out to characterise and compare Saltmarsh and Pasture sites in terms of physicochemical and biological properties.

The introduction of seawater, for increasing lengths of flooding, caused the conductivity and pH values of the soil to become more similar to that of seawater (higher conductivity and pH). Whilst this was not unexpected (Nacke et al., 2017; Taylor and Krüger, 2019; Xian et al., 2019), the results suggest that even a flash flood, mimicked by the 1-h flooding event, can have significant effects on the soil environment. Further, the analysis indicated that the pasture and saltmarsh soils had varying responses to flooding; within saltmarsh soils, conductivity and pH levels are already elevated above the pasture site levels, due to previous seawater inundation (Wang et al., 2014), and remained

somewhat constant throughout the experiment. In pasture mesocosms, conductivity and pH levels increased with flooding duration, potentially because there was no previous exposure to seawater. Previous studies have shown that physicochemical properties (for example pH (Griffiths et al., 2011)) have unified impacts on bacterial composition. The results here, however, indicated no significant association between physicochemical properties and composition, suggesting that there are more complicated interactions at work during these flooding events, which could be mediated by the origin of the mesocosm.

The results indicate that flooding duration does not have a clear effect in terms of compositional shifts. A previous study (García Hernández et al., 2021) indicated that elevation has significant effects on microbial composition, potentially due to exposure to seawater. In this study, there is no clear directional effect, the increase length of flooding does cause an increase in the variance associated with the community composition, however, previous saltwater exposure does explain some of this variation. Previous studies investigating freshwater flooding (González Macé et al., 2016; Graff and Conrad, 2005; Randle-Boggis et al., 2018) have demonstrated that flooding drastically changes microbial composition, however, our results show a more stochastic response. Our results are more consistent with those that investigate seawater flooding (Fitch et al., 2022; Hanley et al., 2020; Rietl et al., 2016) which have also shown there is minimal disruption to the composition over timescales even longer (6 months; (Sjøgaard et al., 2018)) than reported here.

Disturbances in abiotic and biotic conditions can cause communities to demonstrate functional and compositional responses of bacterial communities (Goberna et al., 2014). To better understand the impact of flooding on the carbon cycling potential of the communities, we focused on the activities of two enzymes, xylase (indicative of utilisation of a labile substrate), and cellulase (recalcitrant substrate). Previous studies involving seawater inundation have shown that increasing salinity leads to a reduction of extracellular enzyme activity (Servais et al., 2020; Sinsabaugh et al., 2008). Similarly, our results indicated that there is an overall reduction in enzyme activity, but also a

fundamental shift towards utilising labile substrates with increasing flooding durations. Previous work in aquatic systems indicates that labile substrates are preferentially used during early stages of community assembly, before the community switches towards recalcitrant carbon sources (Rivett et al., 2016). Furthermore, evidence indicates that rarer species are more likely to be responsible for degrading recalcitrant substrates (Rivett and Bell, 2018), which are more likely to be negatively affected by stress (Jousset et al., 2017). This evidence is supported by work conducted on freshwater flooding of soils (Romero-Olivares et al., 2017), with the switch in nutrient utilisation driven by the availability of liable organic matter in soils flooded with seawater (Sjøgaard et al., 2018). This suggests that in the environments studied here, the seawater inundation does not lead to predictable and major shifts in composition but does lead to a shift towards labile substrates as the system recovers.

Importantly, our data also suggest that over the relatively small timescales of storm surges (hours up to 7 days) there is no correlation between the changes in composition and enzyme activity during either the flooding, or recovery, phases of the experiment. This suggests that rather than a community shift causing the changes in ecosystem function, there is a greater possibility that individual bacteria have changed their survival strategies (Aertsen and Michiels, 2004).

To address the question whether previous exposure to seawater stress alters a community's ability to respond to flooding, resistance indices were calculated and suggested that as previous exposure increased (Pasture < High Saltmarsh < Low Saltmarsh) then so did the level of resistance. Previous data have shown that periodic flooding and drainage have shaped the microbiomes within agricultural soils (Gschwend et al., 2020), however, pre-adaptation to stress affords soils some increased protection (Preece et al., 2019).

Interestingly, our results show that after a recovery period, there is a function dependent response with each measured function changing independently. Overall, our results demonstrate that the composition of a community is more likely to transition to an alternative state than recover. This

result is most pronounced in the Low Saltmarsh site, where the composition and all functions measured tended towards an alternative state, rather than recovery. In contrast, the Pasture site was generally shown to recover and thereby showed a greater resilience to the seawater stress than the Saltmarsh sites. This suggests that there is a trade off between the resistance and resilience of the Saltmarsh system and rather than expending energy recovering, those communities with frequent exposure can "flip-flop" between states. Whilst this is in contrast to some macroecological saltmarsh (Castagno et al., 2021) and terrestrial (Bardgett and Caruso, 2020) investigations, this result is precedented within saltmarsh microbiome research (Emery et al., 2019), where community composition is stable in response to the presence of a stressor, with the functionality remaining constant. This would suggest that there is a high level of redundancy in the Saltmarsh communities due to high rates of microbial dormancy (Kearns et al., 2016), which allow the transition to an alternative state (Shade et al., 2012).

4.1. Conclusion

In conclusion, our results demonstrated that seawater flooding significantly impacts soil's physicochemical properties and microbial community composition and functioning. We did not detect a universal direction of change with increasing flooding duration across the compositional or functional measures, suggesting that the changes observed may be specific to individual habitats. One trend that our data indicates is that while an increase in previous exposure to the seawater flooding produces a habitat that is more resistant than naïve sites, there is a reduction in resilience and the movement to an alternate state upon inundation. With flooding events predicted to increase, pertinent questions still need to be addressed concerning the consequences of these alternate states and the wider productivity of the ecosystem.

References

Aertsen and Michiels, 2004

A. Aertsen, C.W. Michiels

Stress and how bacteria cope with death and survival

Crit. Rev. Microbiol., 30 (2004), pp. 263-273

Aguinaga et al., 2018

O.E. Aguinaga, A. McMahon, K.N. White, A.P. Dean, J.K. Pittman

Microbial community shifts in response to acid mine drainage pollution within a natural wetland ecosystem

Front. Microbiol., 9 (2018)

Allison and Martiny, 2008

S.D. Allison, J.B.H. Martiny

Resistance, resilience, and redundancy in microbial communities

Proc. Natl. Acad. Sci., 105 (2008), pp. 11512-11519

Bardgett and Caruso, 2020

R.D. Bardgett, T. Caruso

Soil microbial community responses to climate extremes: resistance, resilience and transitions to alternative states

Phil. Trans. R. Soc. B Biol. Sci., 375 (2020), p. 20190112

Berga et al., 2017

M. Berga, Y. Zha, A.J. Székely, S. Langenheder

Functional and compositional stability of bacterial metacommunities in response to salinity changes

Front. Microbiol., 8 (2017)

Bolyen et al., 2019

E. Bolyen, J.R. Rideout, M.R. Dilon, N.A. Bokulich, C.C. Abnet, G.A. Al-Ghalith, et al.

Reproducible, interative, scalable and extensible microbiome data science using QIIME 2

Nat. Biotechnol., 37 (2019), p. 852

Brown et al., 2021

S. Brown, K. Jenkins, P. Goodwin, D. Lincke, A.T. Vafeidis, R.S.J. Tol, et al.

Global costs of protecting against sea-level rise at 1.5 to 4.0 °C

Clim. Chang., 167 (2021), p. 4

Callahan et al., 2016

B.J. Callahan, P.J. McMurdie, M.J. Rosen, A.W. Han, A.J.A. Johnson, S.P. Holmes

DADA2: high-resolution sample inference from Illumina amplicon data

Nat. Methods, 13 (2016), p. 581

Caporaso et al., 2012

J.G. Caporaso, C.L. Lauber, W.A. Walters, D. Berg-Lyons, J. Huntley, N. Fierer, et al.

Ultra-high-throughput microbial community analysis on the Illumina HiSeq and MiSeq platforms

ISME J., 6 (2012), p. 1621

Castagno et al., 2021

K.A. Castagno, T. Tomiczek, C.C. Shepard, M.W. Beck, A.A. Bowden, K. O'Donnell, et al.

Resistance, resilience, and recovery of salt marshes in the Florida Panhandle following Hurricane Michael

Sci. Rep., 11 (2021), p. 20381

Chambers et al., 2016

L.G. Chambers, R. Guevara, J.N. Boyer, T.G. Troxler, S.E. Davis

Effects of salinity and inundation on microbial community structure and function in a mangrove peat soil

Wetlands, 36 (2016), pp. 361-371

Chaudhary et al., 2016

D.R. Chaudhary, A.P. Rathore, B. Jha

Effects of seawater irrigation on soil microbial community structure and physiological function

Int. J. Environ. Sci. Technol., 13 (2016), pp. 2199-2208

Cheikh and Momen, 2020

M. Cheikh, M. Momen

The Interacting Effects of Storm Surge Intensification and Sea-level Rise on Coastal Resiliency: A High-Resolution Turbulence Resolving Case Study

2 (2020)

Elmholt et al., 2000

S. Elmholt, L.J. Munkholm, K. Debosz, P. Schjønning

Biotic and abiotic binding and bonding mechanisms in soils with long-term differences in management

DIAS Rep., 38 (2000), pp. 53-62

Emery et al., 2019

H.E. Emery, J.H. Angell, R.W. Fulweiler

Salt marsh greenhouse gas fluxes and microbial communities are not sensitive to the first year of precipitation change

J. Geophys. Res. Biogeosci., 124 (2019), pp. 1071-1087

Fitch et al., 2022

A.A. Fitch, K. Blount, L. Reynolds, S.D. Bridgham

Partial recovery of microbial function in restored coastal marshes of Oregon, USA

Soil Sci. Soc. Am. J. (2022), pp. 1-16

Fox and Weisberg, 2019

J. Fox, S. Weisberg

An R Companion to Applied Regression

Sage (2019)

García Hernández et al., 2021

E. García Hernández, M.P. Berg, A.R. Van Oosten, C. Smit, Salles J. Falcão

Linking bacterial communities associated with the environment and the ecosystem engineer orchestia gammarellus at contrasting salt marsh elevations

Microb. Ecol., 82 (2021), pp. 537-548

Glenn et al., 1998

E.P. Glenn, J.J. Brown, J.W. O'Leary

Irrigating crops with seawater

Sci. Am., 279 (1998), pp. 76-81

Goberna et al., 2014

M. Goberna, J.A. Navarro-Cano, A. Valiente-Banuet, C. García, M. Verdú

Abiotic stress tolerance and competition-related traits underlie phylogenetic clustering in soil bacterial communities

Ecol. Lett., 17 (2014), pp. 1191-1201

González Macé et al., 2016

O. González Macé, K. Steinauer, A. Jousset, N. Eisenhauer, S. Scheu

Flood-induced changes in soil microbial functions as modified by plant diversity

PLoS One, 11 (2016), Article e0166349

Gould et al., 2020

I.J. Gould, I. Wright, M. Collison, E. Ruto, G. Bosworth, S. Pearson

The impact of coastal flooding on agriculture: a case-study of Lincolnshire, United Kingdom

Land Degrad. Dev., 31 (2020), pp. 1545-1559

CrossRefView in ScopusGoogle Scholar

Graff and Conrad, 2005

A. Graff, R. Conrad

Impact of flooding on soil bacterial communities associated with poplar (Populus sp.) trees

FEMS Microbiol. Ecol., 53 (2005), pp. 401-415

Griffiths et al., 2011

R.I. Griffiths, B.C. Thomson, P. James, T. Bell, M. Bailey, A.S. Whiteley

The bacterial biogeography of British soils

Environ. Microbiol., 13 (2011), pp. 1642-1654

Gschwend et al., 2020

F. Gschwend, K. Aregger, A. Gramlich, T. Walter, F. Widmer

Periodic waterlogging consistently shapes agricultural soil microbiomes by promoting specific taxa

Appl. Soil Ecol., 155 (2020), p. 103623

Hanley et al., 2020

M.E. Hanley, F.C. Hartley, L. Hayes, M. Franco

Simulated seawater flooding reduces oilseed rape growth, yield and progeny performance

Ann. Bot., 125 (2020), pp. 247-254

Jousset et al., 2017

A. Jousset, C. Bienhold, A. Chatzinotas, L. Gallien, A. Gobet, V. Kurm, et al.

Where less may be more: how the rare biosphere pulls ecosystems strings

ISME J., 11 (2017), pp. 853-862

Kearns et al., 2016

P.J. Kearns, J.H. Angell, E.M. Howard, L.A. Deegan, R.H.R. Stanley, J.L. Bowen

Nutrient enrichment induces dormancy and decreases diversity of active bacteria in salt marsh sediments

Nat. Commun., 7 (2016), p. 12881

Kim, 2019

S. Kim

Storm surges☆

J.K. Cochran, H.J. Bokuniewicz, P.L. Yager (Eds.), Encyclopedia of Ocean Sciences (Third Edition), Academic Press, Oxford (2019), pp. 663-671

Kozich et al., 2013

J.J. Kozich, S.L. Westcott, N.T. Baxter, S.K. Highlander, P.D. Schloss

Development of a dual-index sequencing strategy and curction pipeline for analyzing amplicon sequence data on the MiSeq Illumina sequencing platform

Appl. Environ. Microbiol., 79 (2013), p. 5112

Lee et al., 2016

J.S. Lee, J.-W. Kim, S.H. Lee, H.-H. Myeong, J.-Y. Lee, J.S. Cho

Zonation and soil factors of salt marsh halophyte communities

J. Ecol. Environ., 40 (2016), p. 4

Lombard et al., 2011

N. Lombard, E. Prestat, J.D. van Elsas, P. Simonet

Soil-specific limitations for access and analysis of soil microbial communities by metagenomics

FEMS Microbiol. Ecol., 78 (2011), pp. 31-49

Meena et al., 2017

K.K. Meena, A.M. Sorty, U.M. Bitla, K. Choudhary, P. Gupta, A. Pareek, et al.

Abiotic stress responses and microbe-mediated mitigation in plants: the omics strategies

Front. Plant Sci., 8 (2017)

Mombrikotb et al., 2022

S.B. Mombrikotb, M. Van Agtmaal, E. Johnstone, M.J. Crawley, H.S. Gweon, R.I. Griffiths, et al.

The interactions and hierarchical effects of long-term agricultural stressors on soil bacterial communities

Environ. Microbiol. Rep., 14 (2022), pp. 711-718

Nacke et al., 2017

H. Nacke, I. Schöning, M. Schindler, M. Schrumpf, R. Daniel, G.W. Nicol, et al.

Links between seawater flooding, soil ammonia oxidiser communities and their response to changes in salinity

FEMS Microbiol. Ecol., 93 (2017)

Narayan et al., 2017

S. Narayan, M.W. Beck, P. Wilson, C.J. Thomas, A. Guerrero, C.C. Shepard, et al.

The value of coastal wetlands for flood damage reduction in the northeastern USA

Sci. Rep., 7 (2017), p. 9463

Oksanen et al., 2019

J. Oksanen, F. Guillaume Blanchet, M. Friendly, R. Kindt, P. Legendre, D. McGlinn, et al.

Vegan: Community Ecology Package

(2019)

Orwin and Wardle, 2004

K.H. Orwin, D.A. Wardle

New indices for quantifying the resistance and resilience of soil biota to exogenous disturbances

Soil Biol., 36 (2004), p. 1907

Preece et al., 2019

C. Preece, E. Verbruggen, L. Liu, J.T. Weedon, J. Peñuelas

Effects of past and current drought on the composition and diversity of soil microbial communities

Soil Biol. Biochem., 131 (2019), pp. 28-39

Quast et al., 2013

C. Quast, E. Pruesse, P. Yilmaz, J. Gerken, T. Schweer, P. Yarza, et al.

The SILVA ribosomal RNA gene database project: improved data processing and web-based tools

Nucleic Acids Res., 41 (2013), pp. D590-D596

R CT, 2020

R CT

R: A Language and Environment for Statistical Computing

R Foundation for Statistical Computing (2020)

Randle-Boggis et al., 2018

R.J. Randle-Boggis, P.D. Ashton, T. Helgason

Increasing flooding frequency alters soil microbial communities and functions under laboratory conditions

MicrobiologyOpen, 7 (2018), Article e00548

Rietl et al., 2016

A.J. Rietl, M.E. Overlander, A.J. Nyman, C.R. Jackson

Microbial community composition and extracellular enzyme activities associated with Juncus roemerianus and Spartina alterniflora vegetated sediments in Louisiana saltmarshes

Microb. Ecol., 71 (2016), pp. 290-303

Rivett and Bell, 2018

D.W. Rivett, T. Bell

Abundance determines the functional role of bacterial phylotypes in complex communities

Nat. Microbiol., 3 (2018), pp. 767-772

Rivett et al., 2016

D. Rivett, T. Scheuerl, C. Culbert, S. Mombrikotb, E. Johnstone, T. Barraclough, et al.

Resource-dependent attenuation of species interactions during bacterial succession

ISME J., 10 (2016)

Rogers et al., 2013

G.B. Rogers, L. Cuthbertson, L.R. Hoffman, P.A.C. Wing, C. Pope, D.A.P. Hooftman, et al.

Reducing bias in bacterial community analysis of lower respiratory infections

ISME J., 7 (2013), pp. 697-706

Romero-Olivares et al., 2017

A.L. Romero-Olivares, S.D. Allison, K.K. Treseder

Decomposition of recalcitrant carbon under experimental warming in boreal forest

PLoS One, 12 (2017), Article e0179674

Servais et al., 2020

S. Servais, J.S. Kominoski, C. Coronado-Molina, L. Bauman, S.E. Davis, E.E. Gaiser, et al.

Effects of saltwater pulses on soil microbial enzymes and organic matter breakdown in freshwater and brackish coastal wetlands

Estuar. Coasts, 43 (2020), pp. 814-830

Shade et al., 2012

A. Shade, H. Peter, S. Allison, D. Baho, M. Berga, H. Buergmann, et al.

Fundamentals of microbial community resistance and resilience

Front. Microbiol., 3 (2012)

Sinsabaugh et al., 1991

R.L. Sinsabaugh, R.K. Antibus, A.E. Linkins

Proceedings of the international workshop on modern techniques in soil ecology relevant to organic matter breakdown, nutrient cycling and soil biological processes an enzymic approach to the analysis of microbial activity during plant litter decomposition

Agric. Ecosyst. Environ., 34 (1991), pp. 43-54

Sinsabaugh et al., 2008

R.L. Sinsabaugh, C.L. Lauber, M.N. Weintraub, B. Ahmed, S.D. Allison, C. Crenshaw, et al.

Stoichiometry of soil enzyme activity at global scale

Ecol. Lett., 11 (2008), pp. 1252-1264

Sjøgaard et al., 2018

K.S. Sjøgaard, T.B. Valdemarsen, A.H. Treusch

Responses of an agricultural soil microbiome to flooding with seawater after managed coastal realignment

Microorganisms, 6 (2018), p. 12

Slangen et al., 2016

A.B.A. Slangen, J.A. Church, C. Agosta, X. Fettweis, B. Marzeion, K. Richter

Anthropogenic forcing dominates global mean sea-level rise since 1970

Nat. Clim. Chang., 6 (2016), pp. 701-705

Somboonna et al., 2014

N. Somboonna, A. Wilantho, K. Jankaew, A. Assawamakin, D. Sangsrakru, S. Tangphatsornruang, et al.

Microbial ecology of Thailand tsunami and non-tsunami affected terrestrials

PLoS One, 9 (2014), Article e94236

Taylor and Krüger, 2019

M. Taylor, N. Krüger

Changes in salinity of a clay soil after a short-term salt water flood event

Geoderma Reg., 19 (2019), Article e00239

Wang et al., 2014

Y. Wang, Z.-L. Wang, X. Feng, C. Guo, Q. Chen

Long-term effect of agricultural reclamation on soil chemical properties of a coastal saline marsh in Bohai Rim, Northern China

PLOS ONE, 9 (2014), Article e93727

Warrence et al., 2002

N.J. Warrence, J.W. Bauder, K.E. Pearson

Basics of salinity and sodicity effects on soil physical properties

129, Departement of Land Resources and Environmental Sciences, Montana State University-Bozeman, MT (2002)

Wright et al., 2015

A.J. Wright, A. Ebeling, H. de Kroon, C. Roscher, A. Weigelt, N. Buchmann, et al.

Flooding disturbances increase resource availability and productivity but reduce stability in diverse plant communities

Nat. Commun., 6 (2015), p. 6092

Xian et al., 2019

X. Xian, M. Pang, J. Zhang, M. Zhu, F. Kong, M. Xi

Assessing the effect of potential water and salt intrusion on coastal wetland soil quality: simulation study

J. Soils Sediments, 19 (2019), pp. 2251-2264